IOP PUBLISHING JOURNAL OF PHYSICS D: APPLIED PHYSICS

J. Phys. D: Appl. Phys. **43** (2010) 113001 (14pp) doi:10.1088/0022-3727/43/11/113001

TOPICAL REVIEW

Acoustic cloaking and transformation acoustics

Huanyang Chen[1,2] **and C T Chan**[2]

[1] School of Physical Science and Technology, Soochow University, Suzhou, Jiangsu 215006, People's Republic of China
[2] Department of Physics and the William Mong Institute of NanoScience and Technology, The Hong Kong University of Science and Technology, Clear Water Bay, Hong Kong, People's Republic of China

E-mail: kenyon@ust.hk (H Chen) and phchan@ust.hk (C T Chan)

Received 1 April 2009, in final form 30 January 2010
Published 4 March 2010
Online at stacks.iop.org/JPhysD/43/113001

Abstract
In this review, we give a brief introduction to the application of the new technique of transformation acoustics, which draws on a correspondence between coordinate transformation and material properties. The technique is formulated for both acoustic waves and linear liquid surface waves. Some interesting conceptual devices can be designed for manipulating acoustic waves. For example, we can design acoustic cloaks that make an object invisible to acoustic waves, and the cloak can either encompass or lie outside the object to be concealed. Transformation acoustics, as an analog of transformation optics, can go beyond invisibility cloaking. As an illustration for manipulating linear liquid surface waves, we show that a liquid wave rotator can be designed and fabricated to rotate the wave front. The acoustic transformation media require acoustic materials which are anisotropic and inhomogeneous. Such materials are difficult to find in nature. However, composite materials with embedded sub-wavelength resonators can in principle be made and such 'acoustic metamaterials' can exhibit nearly arbitrary values of effective density and modulus tensors to satisfy the demanding material requirements in transformation acoustics. We introduce resonant sonic materials and Helmholtz resonators as examples of acoustic metamaterials that exhibit resonant behaviour in effective density and effective modulus.

(Some figures in this article are in colour only in the electronic version)

1. Introduction

Recently, the technique of transformation optics [1–5] was introduced to establish a correspondence between material constitutive parameters and coordinate transformations. Such a correspondence enabled people to design conceptual optical components that can control electromagnetic (EM) waves with unprecedented degrees of freedom, resulting in many interesting possibilities. Among all kinds of interesting devices that were derived from transformation optics [6–21], the invisibility cloaking is perhaps the most famous and intriguing [22–35]. Some other transformation media devices [16, 17, 19, 21] also attract some public interest, as evidenced by the numerous reports in the scientific and public media. There are several experimental demonstrations of transformation media devices. In 2006, soon after the first invisibility cloak design based on transformation optics [2] was proposed, a two-dimensional (2D) 'reduced' cloak [23] was realized and fabricated to work in microwave frequencies [22]. A perfect cloaking device can only work at very narrow bandwidth. By sacrificing some scattering cross sections for a wider operation bandwidth [26, 27], one-dimensional (1D) cloak [13] and ground-plane cloak [31] ('invisibility carpet') were later proposed to work in a broader bandwidth. The ground-plane cloak was experimentally demonstrated in microwave frequencies [32] and optical

frequencies [33, 34]. The early transformation optics devices are based on radial transformations in spherical/cylindrical coordinates. Interesting illusion effects can also be obtained using transformation in angular coordinates. For example, a transformation media field rotator based on the transformation optics was proposed [7]. The rotator itself is invisible while the observers inside/outside the rotator would see a rotated world with respect to each other. Later, a reduced form of a broad-band field rotator that can rotate EM wave fronts was realized experimentally by employing a very simple structure comprising an array of identical aluminium metal plates [9]. The recent experimental demonstrations of various forms of transformation media have fuelled their popularity and inspired a great deal of research interest in transformation optics.

Since the transformation optics is based on the invariance of Maxwell's equations under coordinate transformations [36–38], it is natural to explore whether similar techniques can be used to manipulate other kinds of waves. Actually, before the transformation optics was proposed, the direct current (dc) conductivity equation was already shown to be invariant [39, 40] as a corollary of the invariance of Maxwell's equations [36]. A 'push-forward' mapping [39, 40], which expands a point to a circle or sphere, was first proposed to design an anisotropic conductivity that cannot be detected by electrical impedance tomography (EIT). Such a singular mapping is mathematically the same as the transformation media mapping that leads to the famous invisibility cloaking [2]. It was also noted that similar transformation equations appeared in a paper [41] as early as 1961.

The wave equations in most systems do not have such an invariance property. For example, the conventional elastodynamic equations change in form under coordinate transformations [36]. To apply the same spirit of transformation optics, one has to modify the equations of motion [36]. Reference [36] is the first attempt to address the concept of transformation acoustics. If we are lucky enough to find some wave equations that are invariant under coordinate transformations, wave manipulation becomes a geometric problem of finding a proper coordinate transformation. For example, the 2D transformation acoustics was proposed by mapping the acoustic equations to Maxwell's equations of one polarization in the 2D geometry [42]. The acoustic wave equation can also be mapped to the dc conductivity equation, which can be applied to both two and three dimensions and is thus helpful to establish the general principle of transformation acoustics [43]. Similar invariance symmetry was also found in matter waves [44–46]. Both the invariance symmetries for acoustic waves [43] and matter waves [44] come from the invariance symmetry of the scalar Helmholtz equation with a source term [47]. In this review, we will focus on the subject of transformation acoustics [43, 48, 49].

Before the invariance property of the acoustic equation in three dimensions was noted [43], the 2D acoustic cloak problem was already solved [42]. This is possible as the Maxwell equations for one polarization in two dimensions are scalar wave equations, and we just need to find a mapping between corresponding variables. However, such a mapping of variables cannot be applied to three-dimensional (3D) acoustic cloaking because the above equivalence is specific to two dimensions and cannot be generalized to three dimensions [42]. After the invariance symmetry of the acoustic equation was found, a 3D acoustic cloaking [43] was proposed and the transformation acoustics actually goes beyond the ability to design the acoustic cloaking as it can lead to many novel wave manipulation strategies pretty much the same way transformation optics can do for EM waves. It was shown independently that the same results on the 3D acoustic cloaking can be obtained by imposing the requirements of zero scattering effect in the acoustic wave equation [50]. Some subtle issues concerning the acoustic cloaking were also pointed out by various authors [51–55]. In addition to the proposals of passive acoustic cloaking based on the transformation acoustics, which employ various forms of passive metamaterials, there were also papers discussing acoustic cloaking using active sources that either encircle [56] or are external to the object being cloaked [57, 58].

The acoustic cloak designed using radial coordinate transformations has transverse isotropy [59] and can be implemented by layered systems [60–63]. However, the ideal acoustic cloaking using pushing-out type transformation requires extreme material parameters such as infinite mass densities within some parts of the cloaking shell [64] and should be simplified to give more reasonable designs. The process of simplifying the design to achieve more practical implementation is frequently called 'reduction' and the simplified cloaks are called reduced cloaks. There are several proposed reductions of acoustic cloaking [64–67] in the literature following the similar procedures in transformation optics. For practical implementations, various authors have proposed several methods based on employing phononic crystals [61, 68, 69] and acoustic metamaterials [70–74].

There are also works on acoustic cloaks [75, 76] and field rotators [77] for linear liquid surface waves. Although an ideal elastic cloak does not exist due to the non-invariance of the elastic wave equations [36], there are also some works on 'quasi' elastic cloaks [78, 79] that can reduce the scattering cross section of elastic waves for some polarizations. Recently, a layered system was proposed to implement such a 'quasi' elastic cloak [80].

In this review, we will first give an introduction to transformation acoustics in section 2, both for acoustic waves and for linear liquid surface waves. In section 3, we will outline several plausible applications of transformation acoustics, including the internal and external acoustic cloaking for acoustic waves and a field rotator for linear liquid surface waves. In section 4, we will briefly introduce the concept of acoustic metamaterials that would be very useful in future implementations of acoustic transformation media. Finally the conclusions will be given in section 5.

2. Transformation acoustics

Transformation acoustics is based on the invariance of the acoustic wave equation under coordinate transformations [43]. A similar concept could also be applied to linear liquid surface waves [77].

2.1. Acoustic waves

Let us start from the invariance of the conductivity equation [39, 40], which is a corollary of the invariance of Maxwell's equations [36]. Suppose that the potential function $V(x)$ satisfies the conductivity equation [36]

$$\nabla \cdot [\sigma(x)\nabla V(x)] = f(x), \tag{1}$$

where $\sigma(x)$ is the conductivity tensor field and $f(x)$ is the source term. A coordinate transformation is applied to equation (1) from each point x in one space to a corresponding point $x'(x)$ in another space with $V'[x'(x)] = V(x)$. The conductivity equation in the new space can be written as [36]

$$\nabla' \cdot \left[\sigma'(x')\nabla' V'(x')\right] = f'(x'), \tag{2}$$

with $\sigma'(x') = A\sigma(x)A^T/\det A$ and $f'(x') = f(x)/\det A$, where A is the Jacobian transformation matrix with elements, $A_{ki} = \partial x'_k/\partial x_i$.

Now, we write the acoustic equation in the time harmonic form [43],

$$\nabla \cdot \left[\overleftrightarrow{\rho}(x)^{-1}\nabla p(x)\right] = -\frac{\omega^2}{\kappa(x)}p(x), \tag{3}$$

where $\overleftrightarrow{\rho}(x)$ is the mass density tensor distribution, $\kappa(x)$ is the bulk modulus distribution, $p(x)$ is the pressure distribution and ω is the angular frequency. With the variable exchanges [43],

$$[V(x), \sigma(x), f(x)] \Leftrightarrow \left[p(x), \overleftrightarrow{\rho}(x)^{-1}, -\frac{\omega^2}{\kappa(x)}p(x)\right], \tag{4}$$

we can see that the acoustic equation shares the same invariance symmetry with the conductivity equation (1) under coordinate transformations.

Specifically, we apply the coordinate transformation to equation (3) from each point x in one space to a corresponding point $x'(x)$ in another space with $p'[x'(x)] = p(x)$. The acoustic equation in the new space becomes [43]

$$\nabla' \cdot \left[\overleftrightarrow{\rho}'\left(x'\right)^{-1}\nabla' p'\left(x'\right)\right] = -\frac{\omega^2}{\kappa'\left(x'\right)}p'\left(x'\right), \tag{5}$$

where [43]

$$\overleftrightarrow{\rho}'(x')^{-1} = \frac{A\left[\overleftrightarrow{\rho}(x)^{-1}\right]A^T}{\det A}, \qquad \kappa'\left(x'\right) = \det A \times \kappa(x). \tag{6}$$

Here, we should note that $\overleftrightarrow{\rho}'(x')^{-1}$ or $\overleftrightarrow{\rho}(x)^{-1}$ are both tensors, which means that the materials are of transverse isotropy [59]. Equation (6) sets up an equivalent principle for the acoustic materials and the corresponding spatial transformation. The equivalent acoustic materials that can control the flow of acoustic waves in this way in a virtual space are called the 'acoustic transformation media'. The acoustics design based on the coordinate transformation can be referred to as 'transformation acoustics' [48]. We note that in [48], Cummer, Rahm and Schurig used vector scaling to derive the above transformation acoustics equations in orthogonal coordinates.

2.2. Linear liquid surface waves

Let us now turn to the shallow-water wave equation [81] (which is rigorous only in the limit $kh \ll 1$),

$$\nabla \cdot (h\nabla\eta) = -\frac{\omega^2}{g}\eta, \tag{7}$$

where η is the vertical displacement of the water surface, g is the gravitational acceleration, h is the depth of the water and ω is the angular frequency. The dispersion of the linear water surface wave described in the above equation is linear, which is given by $\omega = \sqrt{gh}k$. The propagation of linear water surface waves can in principle be controlled by a distribution in the depth of the water. We will show that a layered structure designed for the depth of the liquid can be obtained by mapping the depth distribution to the permittivity in EM waves. The 'depth' as a function of position can effectively be described by a tensor [77], which shall be called the 'depth tensor'. As shown in the previous subsection, equation (7) has the same invariance property as the acoustic wave equation (or the conductivity equation) under coordinate transformations. If g and h can be arbitrarily chosen, the linear water surface waves could be controlled at will as in the case of acoustics waves and EM waves. However, we should note that g is a factor that cannot be controlled freely. Therefore, we have to limit the above transformation media concept to a subset of coordination transformations that has the condition $\det A = 1$ [13]. The h (or h') is supposed to be anisotropic and position dependent according to the coordination transformations [77],

$$h'(x') = \frac{A[h(x)]A^T}{\det A}. \tag{8}$$

We note that it is a 2D problem here while we were considering a 3D formulation above for the acoustic waves.

3. Applications

There are several applications for the transformation acoustics. The most intriguing possibility is to design an acoustic cloaking shell that can make a domain undetectable by acoustic waves ('inaudible'). In this section, we will give some examples, such as the straightforward application of push-out type mapping to realize 2D and 3D acoustic cloaking. We will show that using acoustic metamaterials with negative modulus and density, we can achieve an acoustic external cloak, which can shield an object from detection, but the cloak does not enclose the object. We will also demonstrate the visual realization of a field rotator that can rotate the wave front of the linear liquid surface waves.

3.1. Acoustic cloaking

Firstly, let us consider the design of acoustic cloaks. Using the same technique as transformation optics in orthogonal coordinates [5], we should have the following transformation acoustic equations in orthogonal coordinates (u', v', w') [43, 48],

$$\overleftrightarrow{\rho}'(u', v', w')^{-1} = \frac{J\left[\overleftrightarrow{\rho}(u, v, w)^{-1}\right]J^T}{\det J},$$
$$\kappa'(u', v', w') = \det J \times \kappa(u, v, w), \tag{9}$$

with the inverse of the density tenors in orthogonal coordinates $\overleftrightarrow{\rho}'(u', v', w')^{-1}$ and $\overleftrightarrow{\rho}(u, v, w)^{-1}$. The mapping is from $(u, v, w) \Leftrightarrow (u', v', w')$, with the Jacobian transformation matrix J written as [5]

$$J = \begin{bmatrix} \frac{h_{u'}}{h_u}\frac{\partial u'}{\partial u} & \frac{h_{u'}}{h_v}\frac{\partial u'}{\partial v} & \frac{h_{u'}}{h_w}\frac{\partial u'}{\partial w} \\ \frac{h_{v'}}{h_u}\frac{\partial v'}{\partial u} & \frac{h_{v'}}{h_v}\frac{\partial v'}{\partial v} & \frac{h_{v'}}{h_w}\frac{\partial w'}{\partial w} \\ \frac{h_{w'}}{h_u}\frac{\partial w'}{\partial u} & \frac{h_{w'}}{h_v}\frac{\partial w'}{\partial v} & \frac{h_{w'}}{h_w}\frac{\partial w'}{\partial w} \end{bmatrix} \tag{10}$$

in orthogonal coordinates, where h_u, h_v, h_w and $h_{u'}, h_{v'}, h_{w'}$ are the scale factors in orthogonal coordinates. For example, let us suppose that $\overleftrightarrow{\rho}(u, v, w)^{-1} = (1/\rho_0)\overleftrightarrow{I}, \kappa(u, v, w) = \kappa_0$ are the parameters of the background, and the mapping is $u' = u'(u), v' = v'(v), w' = w'(w)$. The transformation acoustic equations become [43, 48]

$$\begin{aligned} \overleftrightarrow{\rho}'(u', v', w')^{-1} &= \mathrm{diag}\left\{\frac{1}{\rho_u}, \frac{1}{\rho_v}, \frac{1}{\rho_w}\right\} \\ &= \mathrm{diag}\left\{\frac{Q_u Q_v Q_w}{\rho_0 Q_u^2}, \frac{Q_u Q_v Q_w}{\rho_0 Q_v^2}, \frac{Q_u Q_v Q_w}{\rho_0 Q_w^2}\right\}, \\ \kappa'(u', v', w') &= \frac{\kappa_0}{Q_u Q_v Q_w}, \end{aligned} \tag{11}$$

with

$$\begin{aligned} Q_u &= \frac{h_u}{h_{u'}}\frac{\partial u}{\partial u'}, \\ Q_u &= \frac{h_v}{h_{v'}}\frac{\partial v}{\partial v'}, \\ Q_w &= \frac{h_w}{h_{w'}}\frac{\partial w}{\partial w'}. \end{aligned} \tag{12}$$

We will apply equation (11) to circular cylindrical coordinates and spherical coordinates, and obtain the 2D and 3D acoustic cloaking, respectively.

Similar vector scaling in transformation acoustics has been given in [48], which is based on the original vector scaling analysis in transformation optics [2]. In addition, the scalar Helmholtz equation with a source term is written as [47]

$$\frac{1}{\sqrt{|g|}}\sum_{i,j=1}^{n}\frac{\partial}{\partial x_i}\left(\sqrt{|g|}g^{ij}\frac{\partial p}{\partial x_j}\right) + k^2 p = f, \tag{13}$$

for a Riemannian metric $g = (g_{ij})$ in n-dimensional space, where $|g| = \det(g_{ij})$ and $(g^{ij}) = g^{-1} = (g_{ij})^{-1}$. The connection between this general Helmholtz equation and the acoustic equation is [47]

$$\omega = k, \qquad \overleftrightarrow{\rho}^{-1} = (\sqrt{|g|}g^{ij})/\rho_0, \qquad \kappa = \kappa_0/\sqrt{|g|}, \tag{14}$$

which was first given by Greenleaf *et al* [47, 82]. For example, the corresponding metric tensor from the mapping in orthogonal coordinates is [5]

$$\begin{aligned} g_{ij} &= \mathrm{diag}\left\{\left[\frac{h_u}{h_{u'}}\frac{\partial u}{\partial u'}\right]^2, \left[\frac{h_v}{h_{v'}}\frac{\partial v}{\partial v'}\right]^2, \left[\frac{h_w}{h_{w'}}\frac{\partial w}{\partial w'}\right]^2\right\} \\ &= \mathrm{diag}\left\{Q_u^2, Q_v^2, Q_w^2\right\}, \end{aligned} \tag{15}$$

with $\sqrt{|g|} = Q_u Q_v Q_w$. The same results to equation (11) and (12) can be obtained from the connection with equation (14).

3.1.1. 2D acoustic cloaking. A mapping to produce acoustic cloaking for the cylindrical geometry can be written as $r = f(r'), \theta' = \theta, z' = z$, with [2]

$$f(r') = \begin{cases} r', & r' \geqslant b, \\ \dfrac{b}{b-a}\left(r' - a\right), & a \leqslant r' < b, \end{cases} \tag{16}$$

where a and b are the inner and outer radii of the acoustic cloaking shell. Since the scale factors in circular cylindrical coordinates are $h_r = h_z = 1, h_\theta = r = f(r')$ and $h_{r'} = h_{z'} = 1, h_{\theta'} = r'$, we have

$$\begin{aligned} Q_r &= \frac{h_r}{h_{r'}}\frac{\partial r}{\partial r'} = \frac{b}{b-a}, \\ Q_\theta &= \frac{h_\theta}{h_{\theta'}}\frac{\partial \theta}{\partial \theta'} = \frac{f\left(r'\right)}{r'} = \frac{b}{b-a}\frac{r'-a}{r'}, \\ Q_z &= \frac{h_z}{h_{z'}}\frac{\partial z}{\partial z'} = 1, \end{aligned} \tag{17}$$

and eventually, we have [43]

$$\begin{aligned} \rho_r &= \rho_0\frac{r'}{r'-a}, \\ \rho_\theta &= \rho_0\frac{r'-a}{r'}, \\ \rho_z &= \rho_0\left(\frac{b-a}{b}\right)^2\frac{r'}{r'-a}, \\ \kappa'\left(r', \theta', z'\right) &= \kappa_0\left(\frac{b-a}{b}\right)^2\frac{r'}{r'-a}, \end{aligned} \tag{18}$$

for cylindrical acoustic cloaking. For a 2D acoustic cloaking, the wave vectors have no z-component so that ρ_z is not involved in the early formulation of the problem first given by Cummer and Schurig [42]. In the early version, the acoustic equations in the time-harmonic form [42],

$$\begin{aligned} -\mathrm{i}\omega\rho_\theta v_\theta &= -\frac{1}{r}\frac{\partial p}{\partial \theta}, \\ -\mathrm{i}\omega\rho_r v_r &= -\frac{\partial p}{\partial r}, \\ -\mathrm{i}\omega\frac{p}{\kappa} &= -\frac{1}{r}\frac{\partial\left(r v_r\right)}{\partial r} - \frac{1}{r}\frac{\partial v_\theta}{\partial \theta}, \end{aligned} \tag{19}$$

were mapped to the z-invariant 2D transverse electric (TE) polarized Maxwell equations in circular cylindrical coordinates with the permittivity and permeability tensors (anisotropic and diagonal) [42],

$$\begin{aligned} -\mathrm{i}\omega\mu_r\left(-H_r\right) &= -\frac{1}{r}\frac{\partial\left(-E_z\right)}{\partial \theta}, \\ -\mathrm{i}\omega\mu_\theta H_\theta &= -\frac{\partial\left(-E_z\right)}{\partial r}, \\ -\mathrm{i}\omega\varepsilon_z\left(-E_z\right) &= -\frac{1}{r}\frac{\partial\left(r H_\theta\right)}{\partial r} - \frac{1}{r}\frac{\partial\left(-H_r\right)}{\partial \theta}, \end{aligned} \tag{20}$$

with the variable exchange [42],

$$\left[p, v_r, v_\theta, \rho_r, \rho_\theta, \kappa^{-1}\right] \Leftrightarrow \left[-E_z, H_\theta, -H_r, \mu_\theta, \mu_r, \varepsilon_z\right], \tag{21}$$

where $\vec{v} = v_r\hat{r} + v_\theta\hat{\theta}$ is vector fluid velocity. With known parameters of the 2D EM cloaking [23],

$$\mu_r = \frac{r'-a}{r'}, \qquad \mu_\theta = \frac{r'}{r'-a}, \qquad \varepsilon_z = \left(\frac{b}{b-a}\right)^2 \frac{r'-a}{r'}, \tag{22}$$

the same results to equation (18) for the 2D acoustic cloaking can be obtained. The derivation of these equations follows [42]. More details can be found in the original work. We note that with the choice of $\rho_z = \rho_0((b-a)/b)^2(r'/(r'-a))$, the cylindrical acoustic cloak also functions for waves with oblique incidence.

3.1.2. 3D acoustic cloaking. The same 'push-out' mapping can produce the 3D acoustic cloaking for the spherical geometry. Specifically, the mapping is $r = f(r'), \theta' = \theta$, $\varphi' = \varphi$, with [2]

$$f(r') = \begin{cases} r', & r' \geqslant b, \\ \dfrac{b}{b-a}\left(r'-a\right), & a \leqslant r' < b, \end{cases} \tag{23}$$

where a and b are the inner and outer radii of the 3D acoustic cloaking shell. Since the scale factors in spherical coordinates are $h_r = 1, h_\theta = r = f(r'), h_\varphi = r\sin\theta = f(r')\sin\theta'$ and $h_{r'} = 1, h_{\theta'} = r', h_{\varphi'} = r'\sin\theta'$, we have

$$\begin{aligned} Q_r &= \frac{h_r}{h_{r'}}\frac{\partial r}{\partial r'} = \frac{b}{b-a}, \\ Q_\theta &= \frac{h_\theta}{h_{\theta'}}\frac{\partial\theta}{\partial\theta'} = \frac{f\left(r'\right)}{r'} = \frac{b}{b-a}\frac{r'-a}{r'}, \\ Q_\varphi &= \frac{h_\varphi}{h_{\varphi'}}\frac{\partial\varphi}{\partial\varphi'} = \frac{f\left(r'\right)}{r'} = \frac{b}{b-a}\frac{r'-a}{r'}, \end{aligned} \tag{24}$$

and eventually, we have [43]

$$\begin{aligned} \rho_r &= \rho_0\frac{b-a}{b}\left(\frac{r'}{r'-a}\right)^2, \\ \rho_\theta &= \rho_\varphi = \rho_0\frac{b-a}{b}, \\ \kappa'\left(r',\theta',\varphi'\right) &= \kappa_0\left(\frac{b-a}{b}\right)^3\left(\frac{r'}{r'-a}\right)^2 \end{aligned} \tag{25}$$

for spherical acoustic cloaking (or 3D acoustic cloaking).

In the following, we demonstrate the perfect cloaking effect by directly solving the wave equation using the spherical-Bessel function series expansion method.

Substituting equation (25) into the acoustic equation (5), we have [43]

$$\begin{aligned} &\nabla\cdot\left(\nabla p - \frac{2ar-a^2}{r^2}\frac{\partial p}{\partial r}\hat{r}\right) \\ &\quad = -\frac{\omega^2\rho_0}{\kappa_0}\left(\frac{b}{b-a}\right)^2\left(\frac{r-a}{r}\right)^2 p, \end{aligned} \tag{26}$$

where we drop the primes for aesthetic reasons.

We perform the separation of variables, $p(r,\theta,\varphi) = R(r)\Theta(\theta)\Phi(\varphi)$, the radial part $R(r)$ satisfies [43]

$$\begin{aligned} &\frac{\mathrm{d}}{\mathrm{d}r}\left[(r-a)^2\frac{\mathrm{d}R}{\mathrm{d}r}\right] \\ &\quad + \left[\frac{\omega^2\rho_0}{\kappa_0}\frac{b^2}{(b-a)^2}(r-a)^2 - l(l+1)\right]R = 0. \end{aligned} \tag{27}$$

The general form of the pressure field inside the cloak can thus be expressed as [43]

$$p(r,\theta,\varphi) = \sum_{lm} p_{lm} j_l\left(\sqrt{\frac{\omega^2\rho_0}{\kappa_0}}\frac{b}{b-a}(r-a)\right) Y_l^m(\theta,\varphi), \tag{28}$$

where $Y_l^m(\theta,\varphi)$ are the spherical harmonics and $j_l(x)$ is the lth order spherical Bessel function ($h_l^+(x)$ is the corresponding spherical Hankel function). We note that equation (28) carries no Hankel function due to the singularity at $r = a$. The pressure in $r < a$ can be shown to be zero [27, 29]. For the incident acoustic waves

$$p^0(r,\theta,\varphi) = \sum_{lm} p_{lm}^0 j_l\left(\sqrt{\frac{\omega^2\rho}{\kappa}}\cdot r\right) Y_l^m(\theta,\varphi),$$

we assume that the scattering acoustic waves (for $r \geqslant b$) to be

$$p^+(r,\theta,\varphi) = \sum_{lm} p_{lm}^+ h_l^+\left(\sqrt{\frac{\omega^2\rho}{\kappa}}\cdot r\right) Y_l^m(\theta,\varphi).$$

Substituting them into the boundary conditions at $r = b$ [43],

$$p^+(r=b,\theta,\varphi) + p^0(r=b,\theta,\varphi) = p(r=b,\theta,\varphi), \tag{29}$$

$$\begin{aligned} &\frac{1}{\rho}\left(\frac{\partial p^+}{\partial r}(r=b,\theta,\varphi) + \frac{\partial p^0}{\partial r}(r=b,\theta,\varphi)\right) \\ &\quad = \frac{1}{\rho_r}\frac{\partial p}{\partial r}(r=b,\theta,\varphi), \end{aligned}$$

we have [43]

$$\begin{aligned} &\sum_{lm}\left(p_{lm}^+ h_l^+\left(\sqrt{\frac{\omega^2\rho_0}{\kappa_0}}\cdot b\right) + p_{lm}^0 j_l\left(\sqrt{\frac{\omega^2\rho_0}{\kappa_0}}\cdot b\right)\right) \\ &\quad = \sum_{lm} p_{lm} j_l\left(\sqrt{\frac{\omega^2\rho_0}{\kappa_0}}\cdot b\right), \end{aligned} \tag{30}$$

$$\begin{aligned} &\sum_{lm}\left(p_{lm}^+ h_{l'}^+\left(\sqrt{\frac{\omega^2\rho_0}{\kappa_0}}\cdot b\right) + p_{lm}^0 j_l'\left(\sqrt{\frac{\omega^2\rho_0}{\kappa_0}}\cdot b\right)\right) \\ &\quad \times\sqrt{\frac{\omega^2\rho_0}{\kappa_0}}\frac{1}{\rho_0} = \sum_{lm} p_{lm} j_l'\left(\sqrt{\frac{\omega^2\rho_0}{\kappa_0}}\cdot b\right) \\ &\quad \times\left(\sqrt{\frac{\omega^2\rho_0}{\kappa_0}}\frac{b}{b-a}\right)\left(\frac{b-a}{b}\frac{1}{\rho_0}\right), \end{aligned}$$

that is $p_{lm}^+ = 0$ and $p_{lm} = p_{lm}^0$, which shows that there is no scattering for the 3D acoustic cloaking.

As a concrete example, we suppose that the incident wave is a plane wave in the z-direction with the amplitude p_0 [43],

$$p^0(r,\theta,\varphi) = Re\left[p_0 e^{i\sqrt{\frac{\omega^2\rho}{\kappa}}r\cos\theta}\right], \tag{31}$$

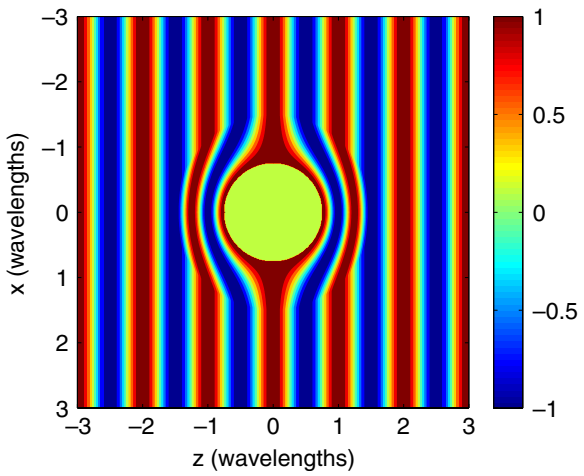

Figure 1. The contour plot of the acoustic pressure field in the x–z plane ($y = 0$) near an incompressible spherical scatterer coated by a 3D acoustic cloaking. Here the unit is λ. See the same results in [43].

then the pressure field inside the cloak should be [43]

$$p(r, \theta, \varphi) = Re\left[p_0 e^{i\sqrt{\frac{\omega^2\rho}{\kappa}}\frac{b}{b-a}(r-a)\cos\theta}\right]. \tag{32}$$

Figure 1 shows the contour plot of the pressure field in the x–z plane ($y = 0$) (see also the figure in the original work [43]). The cloak is designed with $b = 1.5\lambda$ and $a = 0.75\lambda$ for the water background.

By probing the requirements of zero scattering effect in acoustic equation, Cummer *et al* [50] found the material parameters of the spherical acoustic cloaking in an inverse procedure of the above calculation, and the parameters have the same form as equation (25).

3.1.3. Layered designs of acoustic cloaks. In this subsection, we will review how the acoustic cloaking shells could be realized in practice. It has been shown that acoustic materials with transverse isotropic densities could be approximated with alternating thin layers [59]. Using such a concept, ideal acoustic cloaking shells were implemented with layered structures [60, 61]. However, infinite mass density materials are required in such implementations. For that purpose, we need to simplify the material parameters. We will see that an impedance-matched 'reduced' version of the acoustic cloaking shell can be designed whose mass distribution is in a reasonable range [66]. A layered cloak design with isotropic material is also proposed for the reduced cloak.

From equations (18) and (25), we see that the effective density diverges at the inner boundary of the acoustic cloak, which results in the difficult implementation of the devices [64]. Therefore, reduced forms are necessary for practical designs. Before performing the reductions, let us define $\rho_\perp = \rho_\theta$ for the 2D acoustic cloak and $\rho_\perp = \rho_\theta = \rho_\varphi$ for the 3D acoustic cloak. The principal refractive indexes for both the 2D and the 3D acoustic cloak are defined by the ratio of density and bulk modulus and have the same form [66],

$$\frac{n_\perp^2}{n_0^2} = \frac{\rho_\perp/\kappa}{\rho_0/\kappa_0} = \left(\frac{b}{b-a}\right)^2\left(\frac{r-a}{r}\right)^2,$$
$$\frac{n_r^2}{n_0^2} = \frac{\rho_r/\kappa}{\rho_0/\kappa_0} = \left(\frac{b}{b-a}\right)^2. \tag{33}$$

Suppose that κ is a continuous function of r, e.g. $\kappa/\kappa_0 = \kappa(r)$, by keeping the principal refractive indexes, we have [66]

$$\frac{\rho_\perp}{\rho_0} = \kappa(r) \times \left(\frac{b}{b-a}\right)^2\left(\frac{r-a}{r}\right)^2,$$
$$\frac{\rho_r}{\rho_0} = \kappa(r) \times \left(\frac{b}{b-a}\right)^2. \tag{34}$$

The cloaks with the above material parameters are the 'reduced cloaks', which have the same wave bending property of the prefect cloaking, but may have some reflection at the surface, depending on the value of the impedance at the surface. We can choose a proper function $\kappa(r)$ to match the impedances on the outer boundary between the cloak and the background media so that the scattering of an object can be substantially eliminated by the surrounding reduced cloak [30, 83]. For instance, let us choose $\kappa/\kappa_0 = \kappa(r) = (b-a)/b$, the principal values of the density tensor are [66]

$$\frac{\rho_\perp}{\rho_0} = \frac{b}{b-a}\left(\frac{r-a}{r}\right)^2,$$
$$\frac{\rho_r}{\rho_0} = \frac{b}{b-a}, \tag{35}$$

which is finite for all positions and thus more realizable for the actual designs.

In the literature, the transverse isotropic density can be implemented by an alternating layered system [59]. Cheng *et al* [60] use such a system to implement an ideal 2D acoustic cloak with the analogy to the layered design of a non-magnetic reduced EM cloak [84]. The alternating layered system in cylindrical coordinates was shown in figure 2(*a*) (see figure 1(*a*) of [60]). The material in layer A(B) is of density $\rho_A(\rho_B)$ and bulk modulus $\kappa_A(\kappa_B)$. When the thickness of each layer is much smaller than the wavelength, the alternating layered system can be described properly by an effective medium approach and behaves like an effective medium which has the transverse isotropy with its principal axes along the r-direction and θ-direction. The effective principal values of the density tensor and the bulk modulus can be expressed as [59, 60]

$$\rho_r = \frac{\rho_A + \eta\rho_B}{1+\eta},$$
$$\frac{1}{\rho_\theta} = \frac{1}{1+\eta}\left(\frac{1}{\rho_A} + \frac{\eta}{\rho_B}\right), \tag{36}$$
$$\frac{1}{\kappa} = \frac{1}{1+\eta}\left(\frac{1}{\kappa_A} + \frac{\eta}{\kappa_B}\right),$$

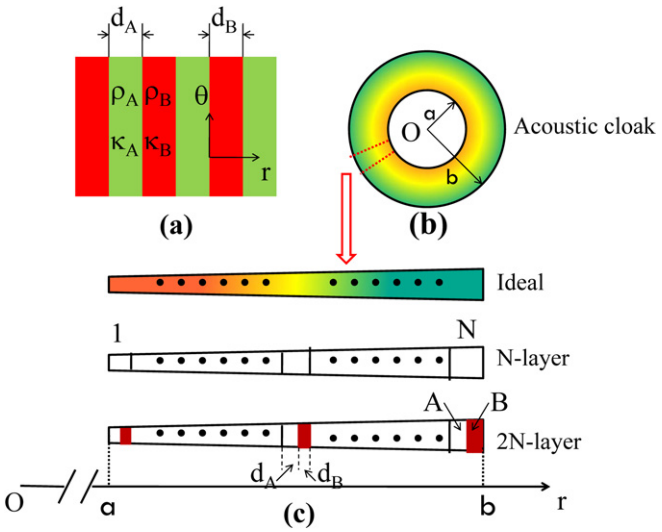

Figure 2. Schematic plot for (*a*) an acoustic layered system; (*b*) an ideal 2D acoustic cloak; (*c*) the design procedure of acoustic cloak with layered system. Adapted from [60], reproduced with permission.

with $\eta(=d_B/d_A)$ the ratio of thicknesses for B layers and A layers.

For an ideal 2D acoustic cloak with its parameters described in equation (18), all parameters are dependent on their radial positions (see figure 2(*b*) or figure 1(*b*) of [60]). To implement such a device, one has to break the cloaking shell into many layers (e.g. N layers) such that each layer possesses a required constant density tensor and a bulk modulus (i.e. the material in each layer is anisotropic but homogeneous, see also [61]). Secondly, as shown in figure 2(*c*) (see figure 1(*c*) of [60]), each layer of anisotropic but homogeneous material can be implemented by the above acoustic alternating layered system with two kinds of isotropic and homogeneous materials. If N is large enough, each layer of anisotropic but homogeneous material can be designed by only two layers of isotropic and homogeneous materials (A and B, see figure 2(*c*) or figure 1(*c*) of [60]). Eventually the cloak can be implemented by $2N$ layers of isotropic and homogeneous materials. Suppose $\eta = 1$, the density and bulk modulus of each layer is [60, 66]

$$\frac{\rho_{2i-1}}{\rho_0} = \frac{r_{2i-1}}{r_{2i-1}-a} - \sqrt{\left(\frac{r_{2i-1}}{r_{2i-1}-a}\right)^2 - 1},$$
$$i = 1, 2, 3, \ldots, N,$$
$$\frac{\rho_{2i}}{\rho_0} = \frac{r_{2i}}{r_{2i}-a} + \sqrt{\left(\frac{r_{2i}}{r_{2i}-a}\right)^2 - 1}, \qquad (37)$$
$$i = 1, 2, 3, \ldots, N,$$
$$\frac{\kappa_i}{\kappa_0} = \left(\frac{b-a}{b}\right)^2 \frac{r_i}{r_i - a}, \qquad i = 1, 2, 3, \ldots, 2\times N,$$

where $r_i = a + ((2i-1)/4N)(b-a)$, $i = 1, 2, 3, \ldots, 2N$.

The calculated acoustic pressure field distribution is shown in figure 3(*a*) (see figure 3(*a*1) of [60]) for an incident plane wave scattered by a rigid cylinder with the radius $a = 1$ m in the water background. Figure 3(*b*) (see figure 3(*a*2) in [60]) shows the pressure field distribution near the cloaking shell with an incident plane wave from left to right. The cloak has 40 layers of isotropic materials ($N = 20$) with the inner and outer radii $a = 1$ m and $b = 2$ m. The working wavelength is set to be $\lambda = 1$ m. Detailed material parameters can be found elsewhere [60]. Figure 3(*b*) (see figure 3(*a*2) in [60]) visually shows that the incident wave is guided around the cloak and reaches the other side of the cloak with little distortion. Similar implementation has been performed to an ideal 3D acoustic cloak [61]. However, for the inner layers, densities and bulk modulus have extreme values. As such, the design is difficult to realize. The aforementioned reduced cloak can play an important role when it is implemented with layered structures. With the parameters of the reduced cloak equation (35) considered, the density and bulk modulus of each

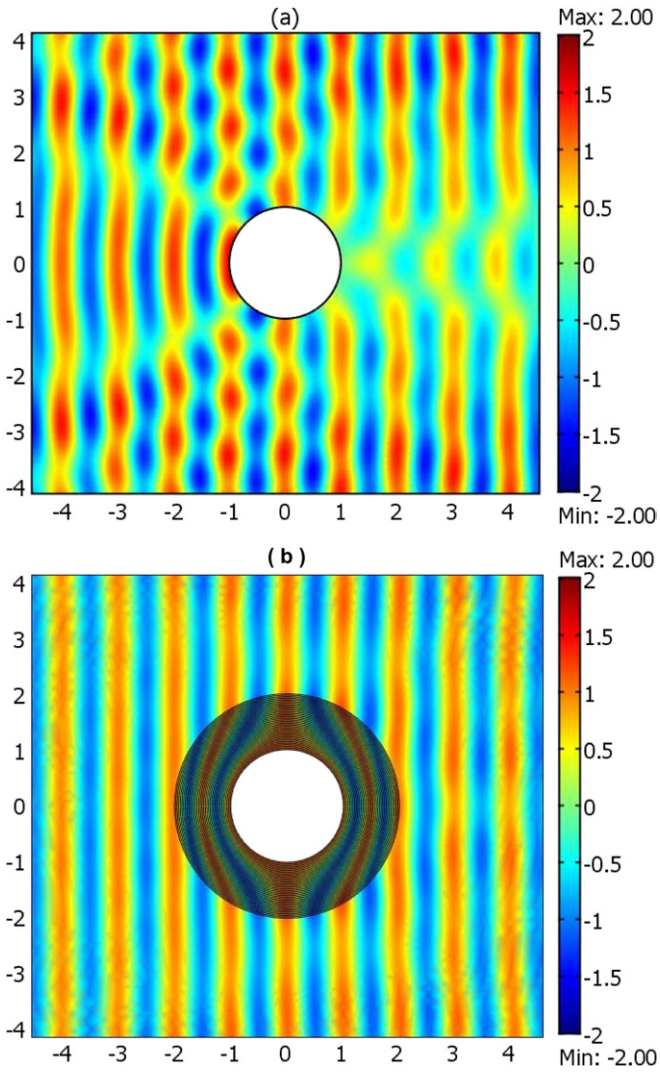

Figure 3. (*a*) The scattering of an acoustic plane wave incident from left to right near a rigid cylinder. (*b*) The acoustic plane wave will be guided smoothly around the rigid cylinder when it is surrounded by the 40-layer acoustic cloak. Adapted from [60], reproduced with permission.

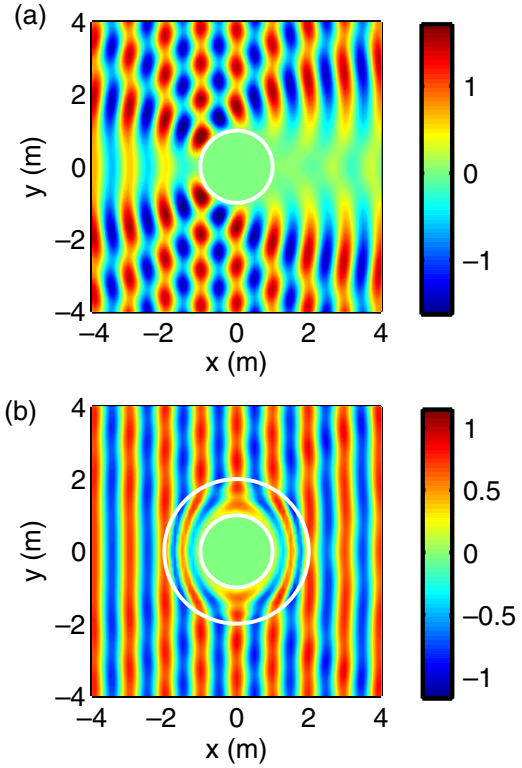

Figure 4. Acoustic wave pressure distribution near an air cylinder (a) without the cloak and (b) with the layered cloak as described in the text. See the same results in [66].

layer become [66]

$$\frac{\rho_{2i-1}}{\rho_0} = \frac{b}{b-a}\left(1-\sqrt{1-\left(\frac{r_{2i-1}-a}{r_{2i-1}}\right)^2}\right), \quad i = 1, 2, 3, \ldots, N, \tag{38}$$

$$\frac{\rho_{2i}}{\rho_0} = \frac{b}{b-a}\left(1+\sqrt{1-\left(\frac{r_{2i}-a}{r_{2i}}\right)^2}\right), \quad i = 1, 2, 3, \ldots, N,$$

and $\kappa_i/\kappa_0 = (b-a)/b, i = 1, 2, 3, \ldots, 2N$. We note that the density ratios ρ_i/ρ_0 are bounded between the range

$$\left[0, \frac{b}{b-a}\left(1-\sqrt{1-\left(\frac{b-a}{b}\right)^2}\right)\right]$$

for the lower density region and between the range

$$\left[\frac{b}{b-a}\left(1+\sqrt{1-\left(\frac{b-a}{b}\right)^2}\right), \frac{2b}{b-a}\right]$$

for the higher density region, which are in a more reasonable range of material parameters.

As a concrete example, we choose to demonstrate the wave scattering properties using the same geometrical parameters and the same working wavelength as in [60]. Figure 4(a) is the calculated acoustic pressure field distribution for an incident plane wave scattered by an air cylinder with the radius $a = 1$ m in the water background [66]. The air cylinder causes great scattering as both the reflection at the front side and the shadow at the back are clearly visible to the eye. By masking the air cylinder with the reduced cloak with a 40-layer design of isotropic materials, the scattering is substantially reduced as shown in figure 4(b) when compared with figure 4(a) [66]. Note that the cloaked object is an air cylinder but not a rigid object used in figure 3 of [60]. The advantage of such a reduced cloak with layered design is very clear. The density ratios are bounded by [0, 0.27] and [3.74, 4], which are more feasible than the ideal case with its density ratios ranging between [0.025, 0.267] and [3.73, 39.99]. The maximum of the density in the reduced cloak is much smaller than that in the ideal one. Therefore the infinite mass singularity no longer exists in the reduced cloak. The reduced cloak with layered structure gives a more feasible design for future implementations. More details can be found in the original work [66].

3.1.4. Acoustic external cloak. In the previous subsections, we have reviewed the conventional acoustic cloaking strategy, which can protect an object inside a quiet interior domain from being detected by an external sonar. The cloaking effect is achieved by steering waves around a domain so that the probing wave can never reach inside the domain. However, such a type of acoustic cloak will also block the signal from any object inside the silent domain, which means that the concealed object is itself deaf to the outside environment. The object cannot hear any sound from outside. In this subsection, we will give an analogy of the EM external cloak [19], which will be called the 'acoustic external cloak'. It can cloak an object without encircling it. In this configuration, the concealed object and the sources are located inside the same domain and the object is exposed to external sound, thereby allowing for the possibility of the object 'hearing' the outside sound sources (by absorbing a small amount of external sound energy).

Because of the close analogy with EM waves, let us start with defining the EM external cloak and see how it works before we discuss the configuration for acoustic waves. Figure 5(a) shows a perfect lens ($\varepsilon' = \mu' = -1$) in the air. The perfect lens and a part of the air to the left of the dashed line form a pair of 'complementary media', a concept first introduced by Pendry and Ramakrishna [85]. The thickness of each slab of complementary media is L. Figure 5(b) shows a generalized form of complementary media including (1) an object with permittivity ε_0 and permeability μ_0 placed to the left of the dashed line inside a layer of air and (2) an 'anti-object' with permittivity $-\varepsilon_0$ and permeability $-\mu_0$ inside the perfect lens. The shape of the 'anti-object' is an image of the object according to the right interface of the perfect lens and the air. The pair of complementary media is optically cancelled by each of its components. A plane wave will pass through it without any phase change as in the case of the perfect lens in figure 5(a). In figure 5(c), a cylindrical lens was obtained after the following coordinate transformation,

$$r = f(r') = \begin{cases} r', & r' \geqslant b, \\ \dfrac{b^2}{r'}, & a \leqslant r' < b, \\ \dfrac{b^2}{a^2}r', & 0 \leqslant r' < a, \end{cases} \tag{39}$$

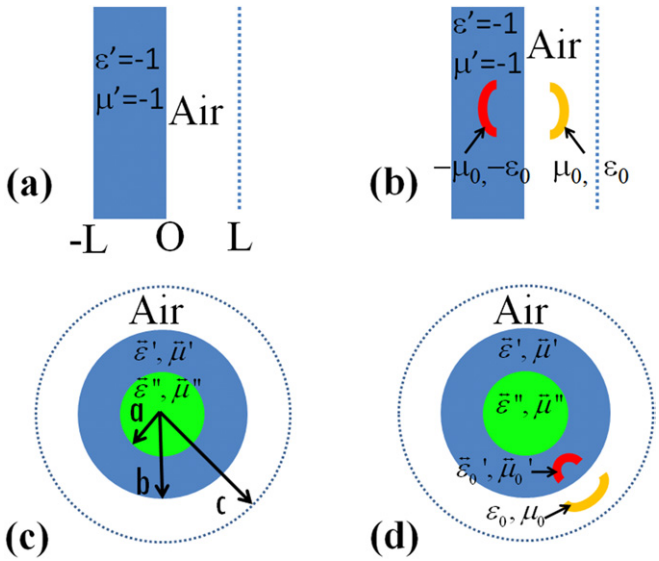

Figure 5. (*a*) A complementary pair of $n = -1$ and $n = 1$ slab forming a perfect lens. (*b*) A complementary media slab with an embedded complementary 'anti-object' that optically cancels an object in air. For a plane wave with k-vector perpendicular to the slab surface, the wave will pass through both configurations (*a*) and (*b*) with zero phase change. For configuration (*b*), the same is true if there are multiple objects and 'anti-objects'. (*c*) Cylindrical lens from equations (39) and (40). The domain inside the dotted circle is equivalent to air. (*d*) This configuration is also equivalent to air for any type of incident wave, as long as the observer is outside the dotted circle. This configuration achieves cloaking at a distance based on the complementary media concept and cylindrical lens. We note that the external object is made invisible by the anti-object embedded inside the cylindrical lens. Figures are adapted from [19].

with $\theta = \theta'$, $z = z'$ and $c = b^2/a$, the permittivity and permeability tensors are thus in the following form,

$$\begin{aligned}\ddot{\varepsilon}(r') &= \ddot{\mu}\left(r'\right)\\ &= \begin{cases} \ddot{I}, & r' \geqslant b,\\ \ddot{\varepsilon}' = \ddot{\mu}' = \mathrm{diag}\left\{-1, -1, -\dfrac{b^4}{r'^4}\right\}, & a \leqslant r' < b,\\ \ddot{\varepsilon}'' = \ddot{\mu}'' = \mathrm{diag}\left\{1, 1, \dfrac{b^4}{a^4}\right\}, & 0 \leqslant r' < a, \end{cases}\end{aligned} \tag{40}$$

in circular cylindrical coordinates. The double negative medium (DNM) in $a \leqslant r' \leqslant b$ and the air in $b \leqslant r' \leqslant c$ form a pair of complementary media in cylindrical coordinates. This complementary pair gives a domain that does not cause any phase change to the incoming wave. In order to mimic air, which does cause phase accumulation, we need to put in some dielectric material in the core $r' < a$, as specified by the last equation in (40). The whole system, including the outer air shell, the DNM, and the core dielectric material, is then optically equal to a circle of air with its radius c, and is thus invisible to any observer outside $r' = c$. If an object of permittivity ε_0 and permeability μ_0 is put in the outer circular shell of air ($b \leqslant r' \leqslant c$), we can perform a similar procedure as in figure 5(*b*) to make it invisible. As shown in figure 5(*d*), an 'anti-object' can be embedded in the DNM shell to make the whole system invisible to the incoming waves outside $r' = c$. The shape of the 'anti-object' is related to the original object following the coordinate transformation. The permittivity and permeability tensors of the 'anti-object' are $\ddot{\varepsilon}_0' = \varepsilon_0 \mathrm{diag}\{-1, -1, -(b^4/r'^4)\}$ and $\ddot{\mu}_0' = \mu_0 \mathrm{diag}\left\{-1, -1, -\left(b^4/r'^4\right)\right\}$ according to the transformation media theory. More details can be found in the original work [19].

As there exists a one-to-one mapping from the z-invariant 2D Maxwell equations for TE polarization to the 2D acoustic wave equations, we can obtain the material parameters of an acoustic external cloak without additional work. It contains three components, the core material, the negative refractive index shell and the embedded 'anti-object'. The core material is isotropic material of density ρ_0 and bulk modulus $(a^4/b^4)\kappa_0$. The negative refractive index shell is isotropic but inhomogeneous material and must be 'double negative' in its constitutive parameters, meaning that it carries a negative effective density $-\rho_0$ and a negative effective bulk modulus $-(r'^4/b^4)\kappa_0$. If the object to be cloaked is of density ρ_1 and bulk modulus κ_1, the material parameters of the 'anti-object' should be of density $-\rho_1$ and bulk modulus $-(r'^4/b^4)\kappa_1$. A similar concept has been applied to a square-shaped device in [86]. The realization of dynamical negative density and negative modulus has been discussed in the literature (see for example section 4).

As an example, let us set the inner and outer radii of the cylindrical lens to be $a = 0.15\,\mathrm{m}$ and $b = 0.216\,\mathrm{m}$. Therefore, the core material is of density ρ_0 and bulk modulus $0.233\kappa_0$. The cloaked object is taken to be a curved sheet of thickness 0.016 m with density ρ_0 and bulk modulus $0.1\kappa_0$ and is positioned between the circles of $r' = 0.255\,\mathrm{m}$ and $r' = 0.271\,\mathrm{m}$. There is in fact no restriction on the shape of the object, and the choice of a curved sheet configuration is for the ease of numerical demonstrations. The 'anti-object' is another curved sheet of thickness 0.011 m with density $-\rho_0$ and bulk modulus $-0.1(r'^4/b^4)\kappa_0$ and is positioned between the circles of $r' = 0.172\,\mathrm{m}$ and $r' = 0.183\,\mathrm{m}$. The working wavelength is set to be 0.15 m. Figure 6(*a*) shows the acoustic pressure field distribution computed using a finite-element package and the results verify the invisibility of the cylindrical lens in figure 5(*c*). Figure 6(*b*) shows the pressure field and confirms the 'external' cloaking effect of the whole system in figure 5(*d*). Without the acoustic external cloak, the curved sheet scatters acoustic waves. Figure 6(*c*) shows its scattering pressure field pattern. Since the required materials are isotropic but position dependent, it can be implemented by layered system.

The acoustic external cloak can cloak an object without encircling it but allow the object to receive signals from the outside environment.

3.2. *Liquid wave rotator*

In this section, we will review an experimental device that can rotate the liquid wave front [77]. As we have shown in section 2.2, if coordination transformations have the condition $\det A = 1$, the transformation media concept can be applied to the linear liquid surface waves and the

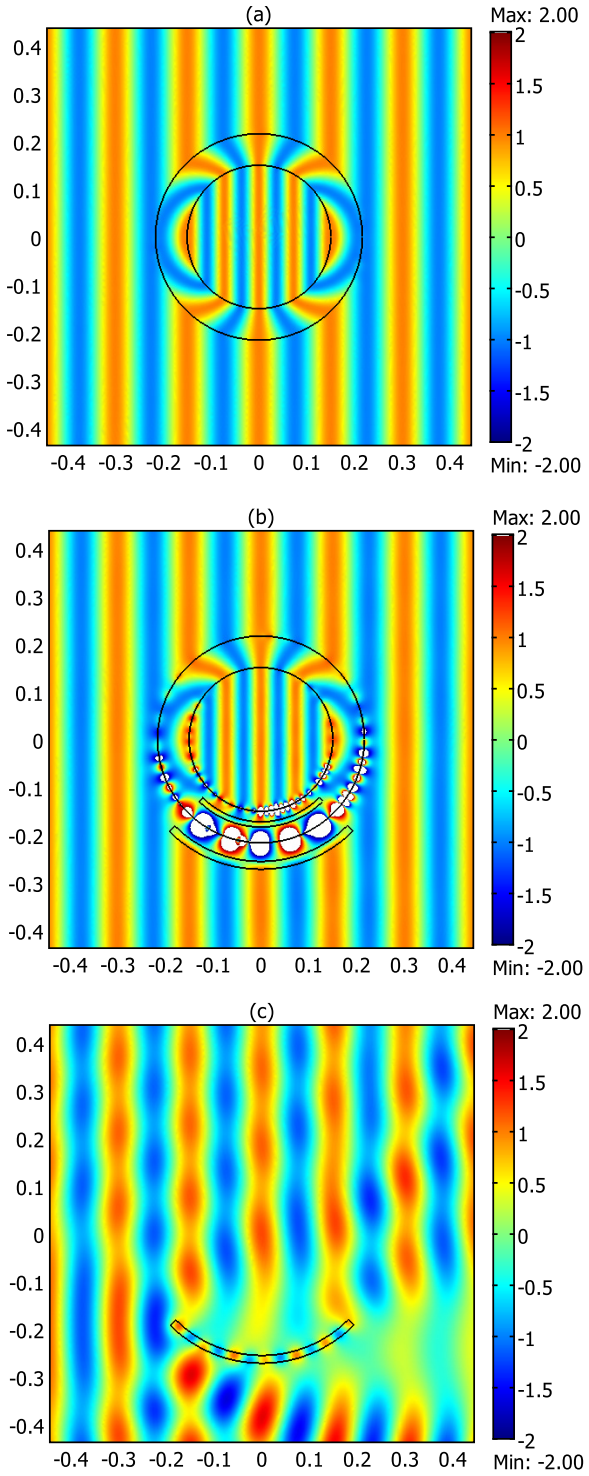

Figure 6. Acoustic pressure distribution near (*a*) an acoustic cylindrical lens; (*b*) an acoustic external cloak; (*c*) a bare scatterer without the external cloak.

implementation requires an anisotropic depth distribution. There are several examples fulfilling such a requirement in transformation optics, including the wave shifter, 1D cloak and wave rotator [13].

Let us now consider the following z-invariant 2D transverse magnetic polarized Maxwell equations with an

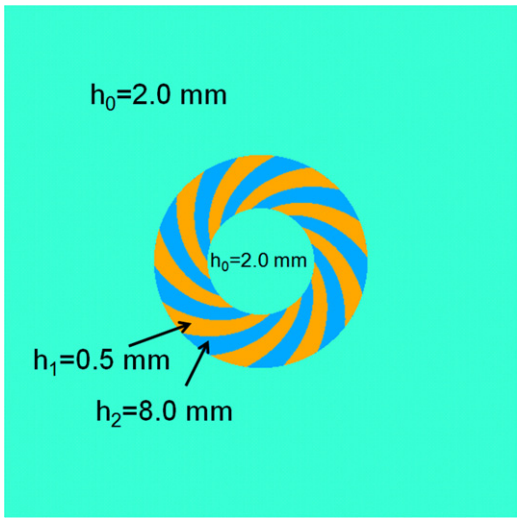

Figure 7. The position dependent depth distribution near the wave rotator of the liquid surface waves. In the actual design, the layered system has 72 layers. For better visualization, we plot a layered system with 18 layers. Adapted from [77].

anisotropic permittivity tensor and no magnetic response [77],

$$\nabla \times \left(\overleftrightarrow{\varepsilon}^{-1} \nabla \times \left(H_z \hat{z}\right)\right) - \mu_0 \varepsilon_0 \omega^2 H_z \hat{z} = 0, \tag{41}$$

which can also be written in another form [77],

$$\nabla \cdot \left(\frac{\overleftrightarrow{\varepsilon}}{\det(\overleftrightarrow{\varepsilon})} \nabla H_z\right) + \mu_0 \varepsilon_0 \omega^2 H_z = 0. \tag{42}$$

There will be a one-to-one mapping between equation (42) and equation (7) ($\overleftrightarrow{\varepsilon}$ is mapped to the anisotropic depth parameter h if $\det(\overleftrightarrow{\varepsilon}) = 1$). The anisotropy of the depth degree of freedom can be implemented using a system of alternating oblique layers. For instance, a wave rotator of the liquid surface waves can be implemented following the layered design in EM waves [13, 77]. The inner and outer radii of the wave rotator are $a = 2.5\,\text{cm}$ and $b = 5.0\,\text{cm}$. The depth outside or inside the rotator is $h_0 = 2.0\,\text{mm}$ [77]. The anisotropic depth parameter in the wave rotator domain can be effectively implemented by two alternating depth distributions with specific geometric shape described in detail in [13] (see figure 7). The alternating depth parameters are $h_1 = 0.5\,\text{mm}$ and $h_2 = 8.0\,\text{mm}$ so that $h_1 \times h_2 = h_0^2$ results in a perfect rotation cloaking effect.

In the numerical simulation, we consider an implementation that contains 72 alternating layers in the rotator domain [77]. A linear liquid surface wave is incident from left to right, with a frequency of 6 Hz. The scattering pattern of the incoming wave interacting with the designed layered wave rotator was plotted in figure 8 as described by equation (7). The rotation angle is about 30.6° from the transformation media theory of the EM field rotators [7, 13], which is consistent with the numerical simulations in figure 8. Note that this wave rotator can function for incoming surface waves with any frequency as long as equation (7) holds at that frequency.

The detailed experimental setup can be found in [77]. Figure 9(*a*) shows the observed scattering wave pattern of the liquid surface waves near the wave rotator. The rotation

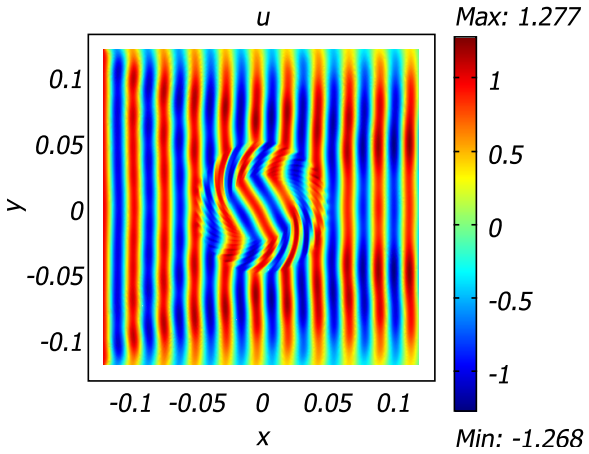

Figure 8. The scattering pattern of an incident surface wave with a frequency of 6 Hz near the rotator. Linear dispersion (see equation (7)) was assumed in the numerical simulations. See the same results in [77].

angle is not the same as that predicted by equation (7) and shown in figure 8. This is because of the nonlinear effect of the liquid surface waves. We note that equation (7) is a rather rough approximation, and it can be modified to include the higher-order terms for a higher accuracy. For a better description, the following nonlinear dispersion should be taken into account [87]:

$$\omega^2 = gk(1 + k^2 d_c^2)\tanh(kh), \tag{43}$$

where d_c is the liquid capillarity length. For a given ω and h, the wave vector k can be obtained by solving the above implicit equation (43) numerically. With the above nonlinear dispersion and higher-order terms being considered, the equation of the liquid surface waves (7) can be written as [88]

$$\nabla \cdot \left(\tilde{h}\nabla\eta\right) = -k^2\tilde{h}\eta, \tag{44}$$

with the effective depth $\tilde{h} = (\tanh(kh)/2k)(1 + (2kh/\sinh(2kh)))$. The above equation with k and $\tilde{h}$ calculated from equation (43) can be solved numerically using finite-element methods. Figure 9(b) shows the simulation results with the nonlinear dispersion relationship included implicitly.

The experimentally observed rotation angles agree with the simulation reasonably well when we compare figures 9(a) and (b). Moreover, both results show little backward scattering. However, the experimental result shows a shadow behind the wave rotator, which is due to the dissipation of the liquid surface waves [75]. The rotator has fairly broad-band functionality because the transformation mapping is not singular. More details can be found in the original work [77].

Recently, a cloak for linear liquid surface waves [75] was also designed using a different method rather than the above transformation acoustics, which generates great public interest.

4. Acoustic metamaterial implementations

Since acoustic transformation media require anisotropic and inhomogeneous density and inhomogeneous bulk modulus, it

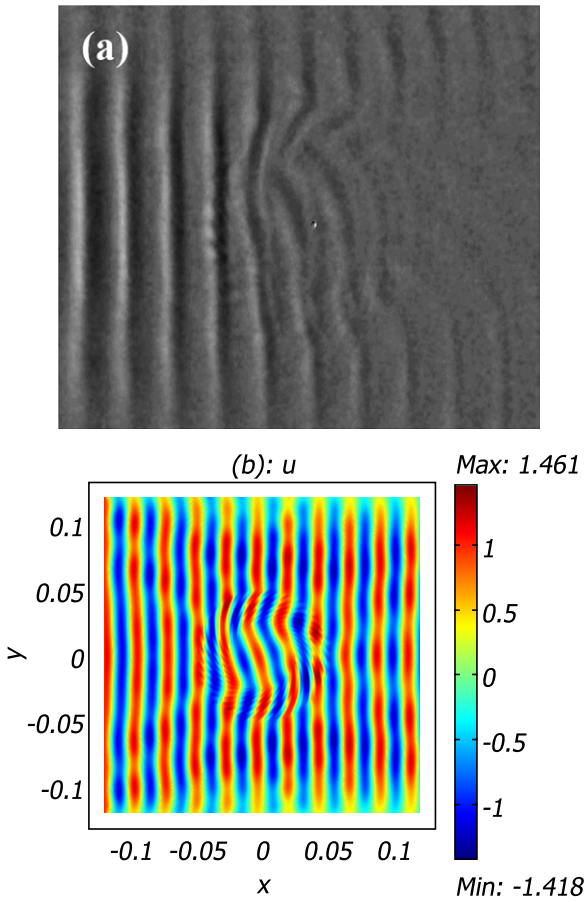

Figure 9. (a) The observed scattering pattern of liquid surface waves near the wave rotator. The frequency is 6 Hz. (b) The calculated scattering pattern when the dispersion relationship (equation (43)) is considered. See the same results in [77].

is very challenging to implement such material parameters. Elastic transformation media can exist only for some polarizations of elastic waves and are more difficult to implement than the acoustic one [78, 79]. To implement the transverse anisotropic density, one possibility is to employ the aforementioned layered system of alternating isotropic materials. The phononic crystals are another feasible choice to obtain the transverse anisotropic density [61, 68, 69], which will not be discussed in detail here. Usually, the alternating layered system contains many kinds of isotropic materials, which should be designed using acoustic metamaterials. The acoustic metamaterials are man-made materials with small embedded artificial resonators which can give nearly any value of effective density or bulk modulus. In this section, we will briefly discuss the physical meaning of negative density [70] or negative bulk modulus [72] and how they may be realized in principle. They should be good candidates for future implementations of acoustic transformation media.

While the notion of a 'negative mass' may sound strange, it is actually not difficult to understand if we examine the following example. Let us start from a 1D spring–mass model that is frequently used in solid state textbooks. The model is illustrated in figure 10(a) schematically. The solution of the eigenfrequency of this simple model is given by $\omega^2 = 4KM^{-1}\sin^2(ka/2)$, where K is the spring constant, M is the

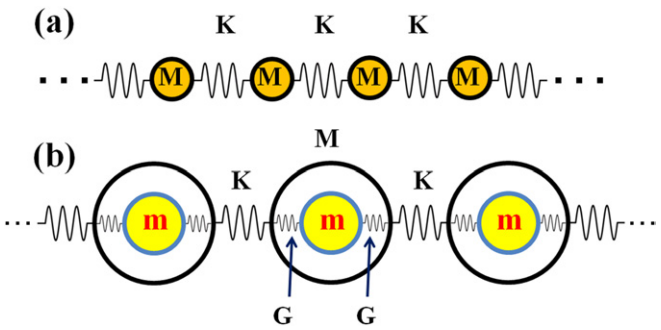

Figure 10. Schematic structure of (*a*) a simple textbook spring–mass model, (*b*) a spring–mass model with internal resonating structures. Adapted from [90], see similar schematic plots in [92].

mass of each ball, k is the wave vector and a is the lattice constant of the system. This solution can be regarded as a dispersion relation, which is analogous to the EM wave case given by $k^2 = \varepsilon\mu\varepsilon_0\mu_0\omega^2$. Usually, M and K are positive. Is it possible to make one of them (e.g. M) negative? The answer is yes if the resonance structures are included [89–92]. Let us consider a more complex system which is illustrated in figure 10(*b*). The balls of mass M in figure 10(*a*) are replaced by locally resonant building blocks. Each block contains a core with mass m connected internally to a shell with mass M through two springs with spring constant G. The dispersion relation for such a system is $\omega^2 = 4KM_{\text{eff}}^{-1}\sin^2(ka/2)$ with the effective mass $M_{\text{eff}} = M + m\omega_0^2/(\omega_0^2 - \omega^2)$, where $\omega_0 = \sqrt{2G/m}$. Near the resonance frequency ω_0, the effective mass could be negative, which means that the response is out of phase with the input force. The similar conceptual spring models of the negative density can also be found in [92].

Real samples that are very similar to this model with a negative effective mass have actually been made and measured. Liu *et al* [70] showed that the locally resonant sonic materials (LRSMs) can exhibit spectral gaps with a lattice constant that is much smaller than the relevant wavelength. The LRSM was later shown to exhibit negative effective density in the band gap frequencies using the effective medium method which obtains effective parameters of a two-component composite from multiple scattering techniques. The units of the original LRSM are lead balls as the core material coated with a layer of silicone rubber (see figure 11). The epoxy was used as the hard matrix material. The resonance in such a structure is derived inherently from the dipolar resonance ($m = 1$ [93]) which can also be seen clearly in the above modified spring model. The core material would be moving opposite in phase to the incident waves in the matrix in the negative effective density frequency range. Such materials can be treated as a usual component for the acoustic metamaterials. The operation of such a negative mass LRSM can be easily understood if we associate the lead balls, the silicone rubber and the epoxy in the LRSM with the small mass m, the inner force spring G and the external spring K in the ball-and-spring system depicted in figure 10. Negative effective mass can also be realized using resonances in certain membrane type structures [71, 94].

Later on, negative effective bulk modulus was also realized by using Helmholtz resonators [73, 95], which is derived from

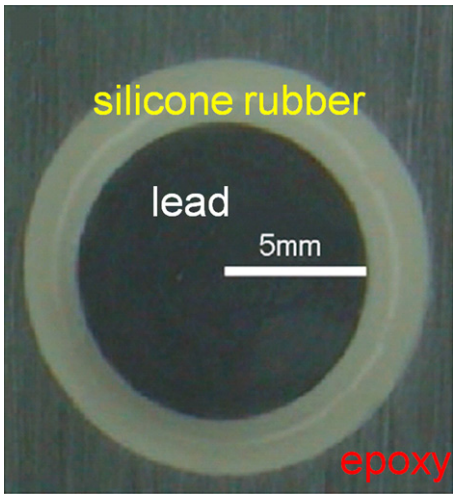

Figure 11. A cross-section picture taken for LRSMs with the units consisting of lead balls as the core material coated with a layer of silicone rubber, and locating in epoxy as the background. Adapted from [70].

a monopolar resonance ($m = 0$ [73]). With the possibility of realizing negative density and effective modulus, double negative acoustic metamaterials with both negative density and bulk modulus would be realizable. It is of course not obvious whether the negative density and negative modulus can be realized in the same frequency range, and if so, whether we can still use an effective medium description in a meaningful manner. The problem was solved [72], and it was found explicitly that in a two-component system with rubber spheres in water, the monopolar and dipolar resonance can give rise to negative effective modulus and negative effective density in the same frequency range, and in addition, the system can be accurately described by an effective medium description. Reference [72] also generalized effective medium theory results so that they can work close to a resonance, and the new effective medium formulae show that the modulus is related to monopolar resonance and the density is related to dipolar resonance. As long as one can find a system in which the monopolar resonance and the dipolar resonance occur in the same frequency range, one can realize 'double negative' acoustic metamaterials. Recently, an acoustic metamaterial lens composed of a planar network of sub-wavelength Helmholtz resonators was designed and gave high-resolution acoustic imaging experimentally due to the negative effective modulus and negative effective density in the kilohertz frequency range [74]. Similar designs might be applied to other acoustic transformation media in future.

5. Conclusions

We have reviewed the recent progress of the transformation acoustics, both for acoustic waves and for linear liquid surface waves. The acoustic interior cloaking and the acoustic external cloaking were discussed as examples for acoustic waves. The interior cloaking is achieved by steering waves around an object, while exterior cloaking is achieved by wave scattering cancellation employing the concept of

complementary media. Concealing objects is only one application of the transformation media concept, which can be used to design different types of conceptual devices to manipulate waves in a very flexible manner. To demonstrate other acoustic wave manipulation ability of the transformation media concept, we have shown that a liquid wave rotator can be fabricated for linear liquid surface waves. The acoustic transformation media require acoustic materials with rather unusual values of densities and modulus. Such material can be realized based on the recent progress of acoustic metamaterial [72]. We outlined two kinds of them (LSRM and Helmholtz resonators) as examples.

Acknowledgments

This work was supported by the Hong Kong RGC General Research Fund #600209. Computation resources were supported by the Shun Hing Education and Charity Fund.

References

[1] Leonhardt U 2006 *Science* **312** 1777
[2] Pendry J B, Schurig D and Smith D R 2006 *Science* **312** 1780
[3] Leonhardt U and Philbin T G 2009 *Prog. Opt.* **53** 69–152
[4] Greenleaf A, Kurylev Y, Lassas M and Uhlmann G 2009 *SIAM Rev.* **51** 3
[5] Chen H 2009 *J. Opt. A: Pure Appl. Opt.* **11** 075102
[6] Rahm M, Schurig D, Roberts D A, Cummer S A, Smith D R and Pendry J B 2008 *Photon. Nanostruct. Fundam. Appl.* **6** 87
[7] Chen H Y and Chan C T 2007 *Appl. Phys. Lett.* **90** 241105
[8] Luo Y, Chen H S, Zhang J, Ran L and Kong J A 2008 *Phys. Rev.* B **77** 125127
[9] Chen H Y, Hou B, Chen S, Ao X, Wen W and Chan C T 2009 *Phys. Rev. Lett.* **102** 183903
[10] Greenleaf A, Kurylev Y, Lassas M and Uhlmann G 2007 *Phys. Rev. Lett.* **99** 183901
[11] Kildishev A V and Narimanov E E 2007 *Opt. Lett.* **32** 3432
[12] Rahm M, Cummer S A, Schurig D, Pendry J B and Smith D R 2008 *Phys. Rev. Lett.* **100** 063903
[13] Chen H Y and Chan C T 2008 *Phys. Rev.* B **78** 054204
[14] Chen H Y, Luo X, Ma H and Chan C T 2008 *Opt. Express* **16** 14603
[15] Yan M, Yan W and Qiu M 2008 *Phys. Rev.* B **78** 125113
[16] Yang T, Chen H Y, Luo X and Ma H 2008 *Opt. Express* **16** 18545
[17] Luo X, Yang T, Gu Y, Chen H Y and Ma H 2009 *Appl. Phys. Lett.* **94** 223513
[18] Ng J, Chen H Y and Chan C T 2009 *Opt. Lett.* **34** 644
[19] Lai Y, Chen H Y, Zhang Z Q and Chan C T 2009 *Phys. Rev. Lett.* **102** 093901
[20] Chen H Y, Chan C T, Liu S and Lin Z 2009 *New J. Phys.* **11** 083012
[21] Lai Y, Ng J, Chen H Y, Han D Z, Xiao J J, Zhang Z-Q and Chan C T 2009 *Phys. Rev. Lett.* **102** 253902
[22] Schurig D, Mock J J, Justice B J, Cummer S A, Pendry J B, Starr A F and Smith D R 2006 *Science* **314** 977
[23] Cummer S A, Popa B-I, Schurig D, Smith D R and Pendry J B 2006 *Phys. Rev.* E **74** 036621
[24] Schurig D, Pendry J B and Smith D R 2006 *Opt. Express* **14** 9794
[25] Cai W, Chettiar U K, Kildishev A V and Shalaev V M 2007 *Nature Photon.* **1** 224
[26] Chen H Y, Liang Z, Yao P, Jiang X, Ma H and Chan C T 2007 *Phys. Rev.* B **76** 241104(R)
[27] Kildishev A V, Cai W, Chettiar U K and Shalaev V M 2008 *New J. Phys.* **10** 115029
[28] Chen H, Wu B-I, Zhang B and Kong J A 2007 *Phys. Rev. Lett.* **99** 063903
[29] Ruan Z, Yan M, Neff C W and Qiu M 2007 *Phys. Rev. Lett.* **99** 113903
[30] Cai W, Chettiar U K, Kildishev A V, Shalaev V M and Milton G W 2007 *Appl. Phys. Lett.* **91** 111105
[31] Li J and Pendry J B 2008 *Phys. Rev. Lett.* **101** 203901
[32] Liu R, Ji C, Mock J J, Chin J Y, Cui T J and Smith D R 2009 *Science* **323** 366
[33] Valentine J, Li J, Zentgraf T, Bartal G and Zhang X 2009 *Nature Mater.* **8** 568
[34] Gabrielli L H, Cardenas J, Poitras C B and Lipson M 2009 *Nature Photon.* **3** 461
[35] Leonhardt U and Tyc T 2009 *Science* **323** 110
[36] Milton G W, Briane M and Willis J R 2006 *New J. Phys.* **8** 248
[37] Weyl H 1921 *Raum–Zeit–Materie (Space–Time–Matter)* 4th edn (Berlin: Springer)
[38] Post E J 1962 *Formal Structure of Electromagnetics: General Covariance and Electromagnetics* (New York: Wiley)
[39] Greenleaf A, Lassas M and Uhlmann G 2003 *Math. Res. Lett.* **10** 685
[40] Greenleaf A, Lassas M and Uhlmann G 2003 *Physiol. Meas.* **24** 413
[41] Dolin L S 1961 *Izv. Vyssh. Uchebn. Zaved. Radiofiz.* **4** 964
[42] Cummer S A and Schurig D 2007 *New J. Phys.* **9** 45
[43] Chen H Y and Chan C T 2007 *Appl. Phys. Lett.* **91** 183518
[44] Zhang S, Genov D A, Sun C and Zhang X 2008 *Phys. Rev. Lett.* **100** 123002
[45] Greenleaf A, Kurylev Y, Lassas M and Uhlmann G 2008 *Phys. Rev. Lett.* **101** 220404
[46] Lin D-H and Luan P-G 2009 *Phys. Rev.* A **79** 051605
[47] Greenleaf A, Kurylev Y, Lassas M and Uhlmann G 2008 arXiv:physics/0801.3279
[48] Cummer S A, Rahm M and Schurig D 2008 *New J. Phys.* **10** 115025
[49] Norris A N 2009 *J. Acoust. Soc. Am.* **125** 839
[50] Cummer S A, Popa B-I, Schurig D, Smith D R, Pendry J B, Rahm M and Starr A 2008 *Phys. Rev. Lett.* **100** 024301
[51] Cai L-W and Sanchez-Dehesa J 2007 *New J. Phys.* **9** 450
[52] Cheng Y and Liu X J 2008 *Appl. Phys. Lett.* **93** 071903
[53] Cheng Y and Liu X J 2008 *J. Appl. Phys.* **104** 104911
[54] Kohn R, Onofrei D, Vogelius M and Weinstein M 2009 *Commun. Pure Appl. Math.* (see also in http://www.math.nyu.edu/faculty/kohn/papers/kohn-onofrei-vogelius-weinstein.pdf) at press
[55] Liu H 2009 *Inverse Problems* **25** 045006
[56] Miller D A B 2006 *Opt. Express* **14** 12457
[57] Vasquez F G, Milton G W and Onofrei D 2009 *Phys. Rev. Lett.* **103** 073901
[58] Vasquez F G, Milton G W and Onofrei D 2009 *Opt. Express* **17** 14800
[59] Schoenberg M and Sen P N 1983 *J. Acoust. Soc. Am.* **73** 61
[60] Cheng Y, Yang F, Xu J Y and Liu X J 2008 *Appl. Phys. Lett.* **92** 151913
[61] Torrent D and Sanchez-Dehesa J 2008 *New J. Phys.* **10** 063015
[62] Cheng Y and Liu X J 2009 *Appl. Phys.* A **94** 25
[63] Greenleaf A, Kurylev Y, Lassas M and Uhlmann G 2008 *New J. Phys.* **10** 115024
[64] Norris A N 2008 arXiv:physics/0802.0701
[65] Norris A N 2008 *Proc. R. Soc. Lond. Ser.* A **464** 2411
[66] Chen H Y, Yang T, Luo X and Ma H 2008 *Chin. Phys. Lett.* **25** 3696
[67] Pendry J B and Li J 2008 *New J. Phys.* **10** 115032
[68] Torrent D and Sanchez-Dehesa J 2008 *New J. Phys.* **10** 023004
[69] Mei J, Liu Z, Wen W and Sheng P 2006 *Phys. Rev. Lett.* **96** 024301

[70] Liu Z, Zhang X, Mao Y, Zhu Y Y, Yang Z, Chan C T and Sheng P 2000 *Science* **289** 1734
[71] Yang Z, Mei J, Yang M, Chan N H and Sheng P 2008 *Phys. Rev. Lett.* **101** 204301
[72] Li J and Chan C T 2004 *Phys. Rev.* E **70** 055602
[73] Fang N, Xi D J, Xu J Y, Ambati M, Sprituravanich W, Sun C and Zhang X 2006 *Nature Mater.* **5** 452
[74] Zhang S, Yin L and Fang N 2009 *Phys. Rev. Lett.* **102** 194301
[75] Farhat M, Enoch S, Guenneau S and Movchan A B 2008 *Phys. Rev. Lett.* **101** 134501
[76] Farhat M, Guenneau S, Enoch S, Movchan A, Zolla F and Nicolet A 2008 *New J. Phys.* **10** 115030
[77] Chen H Y, Yang J, Zi J and Chan C T 2009 *Europhys. Lett.* **85** 24004
[78] Farhat M, Guenneau S, Enoch S and Movchan A B 2009 *Phys. Rev.* B **79** 033102
[79] Brun M, Guenneau S and Movchan A B 2009 *Appl. Phys. Lett.* **94** 061903
[80] Farhat M, Guenneau S and Enoch S 2009 *Phys. Rev. Lett.* **103** 024301
[81] Dingemans M W 1997 *Water Wave Propagation over Uneven Bottoms* (Singapore: World Scientific)
[82] Greenleaf A, Kurylev Y, Lassas M and Uhlmann G 2007 *Commun. Math. Phys.* **275** 749
[83] Yan M, Ruan Z and Qiu M 2007 *Opt. Express* **15** 17772
[84] Huang Y, Feng Y and Jiang T 2007 *Opt. Express* **18** 11133
[85] Pendry J B and Ramakrishna S A 2003 *J. Phys. Condens. Matter* **15** 6345
[86] Liu B and Huang J P 2009 *Eur. Phys. J. Appl. Phys.* **48** 1
[87] Acheson D J 1990 *Elementary Fluid Dynamics* (Oxford: Oxford University Press)
[88] Hu X H, Shen Y F, Liu X H, Fu R T and Zi J 2003 *Phys. Rev.* E **68** 066308
[89] Fung K H, Liu Z and Chan C T 2005 *Z. Kristallogr.* **220** 871
[90] Chan C T, Li J and Fung K H 2006 *J. Zhejiang Univ. Sci.* A **7** 24
[91] Li J, Fung K H, Liu Z Y, Sheng P and Chan C T 2007 *Physics of Negative Refraction and Negative Index Materials* ed C M Krowne and Y Zhang (Berlin: Springer) pp 183–215
[92] Milton G W and Willis J R 2007 *Proc. R. Soc. Lond.* A **463** 855
[93] Liu Z Y, Chan C T and Sheng P 2005 *Phys. Rev.* B **71** 014103
[94] Lee S H, Park C M, Seo Y M, Wang Z G and Kim C K 2009 *Phys. Lett.* A **373** 4464
[95] Lee S H, Park C M, Seo Y M, Wang Z G and Kim C K 2009 *J. Phys.: Condens. Matter* **21** 175704